A two-stage observer for the compensation of actuator-induced disturbances in tool-force sensors

authored by **U. Knechtelsdorfer, M. Saxinger, M. Schwegel, A. Steinboeck, and A. Kugi**

and published in *Mechanical Systems and Signal Processing*.

Contact:

Automation and Control Institute (ACIN)
TU Wien
Gusshausstrasse 27-29/E376
1040 Vienna, Austria

Internet: www.acin.tuwien.ac.at
E-mail: office@acin.tuwien.ac.at
Phone: +43 1 58801 37601
Fax: +43 1 58801 37699

A Two-Stage Observer for the Compensation of Actuator-Induced Disturbances in Tool-Force Sensors

U. Knechtelsdorfer[a,*], M. Saxinger[a], M. Schwegel[b], A. Steinboeck[b], A. Kugi[a]

[a] *Christian Doppler Laboratory for Model-Based Process Control in the Steel Industry, Automation and Control Institute, TU Wien, Gußhausstraße 27-29/376, 1040 Vienna, Austria*
[b] *Automation and Control Institute, TU Wien, Gußhausstraße 27-29/376, 1040 Vienna, Austria*

Abstract

In this paper, a novel two-stage observer strategy for improving the measurement of tool forces is presented. The mass-spring-damper system which inevitably occurs when a tool and a (compliant) force sensor are combined is studied and its adverse influence on the measurement signal is analyzed. The proposed observer consists of two stages. The first stage captures the input-output characteristics from the control input to the tool force by a recursive least-squares estimation algorithm. The estimated tool characteristics are used in a second stage to suppress the oscillations in the measurement signal, which mainly occur due to the mass-spring-damper nature of the tool-sensor combination. In a tailored experimental test rig, which mimics the conditions in magnetic levitation, magnetic bearings, or magnetic strip positioning devices in hot-dip galvanizing lines, the efficacy and the high estimation accuracy of the developed observer strategy are demonstrated.

Keywords: Sensor response correction, Model based disturbance observer, Tool force sensor, Reduced Luenberger observer, Model adaption, Measurement results

1. Introduction

The dynamic measurement of the true tool or actuator forces is a challenging field of research. Real (non-ideal) force sensors often suffer from unwanted effects due to their internal design, e.g., friction, damping, and inertia forces [1]. Furthermore, a force sensor cannot be mounted such that the measurement is not disturbed by the actuator itself. This issue is well studied in the literature, see, e. g., [2, 3, 4, 5, 6, 7, 8, 9, 10].

The disturbances occurring in the measurement of the cutting forces in a mill can be compensated by Kalman filtering as proposed in [2, 3], transfer function inversion [4, 5], or by sensorless estimation [6].

In the field of robotics the measurement of manipulator forces is the topic of many scientific publications. For example, the pre-planned robot trajectory is used for the compensation of the disturbances induced by the inertia of the end effector in [7] and a sensor fusion approach is presented in [8]. In [11] inverse filtering is applied to a transfer function which is identified with respect to the robot's joint configuration. A reaction force observer was developed for sensorless force estimation in [12]. This approach was extended in [13] to consider the environment by means of an adaptive spring model. Another sensorless approach using a sliding-mode observer is presented in [14].

Force sensors are also used in gravimetric mass measurement. In this application, dynamic force measurement can speed up the weighing process because the waiting time for the oscillations to decay is avoided. For this, adaptive filters [9, 10, 15], time-variant filters [16], and neural networks [17] are used. Furthermore, a technique similar to the pre-shaping of control signals, see, e. g., [18], can be used to suppress disturbances due to mechanical oscillations in the force measurement [19].

Generally, if a force is applied by an actuator or an actuated tool, the control input of the actuator is usually known, e. g., the current of an electromagnetic actuator. This a-priori knowledge (e. g., in [7] and [8] the robot movement)

*Corresponding author
Email address: knechtelsdorfer@acin.tuwien.ac.at (U. Knechtelsdorfer)

Post-print version of the article: U. Knechtelsdorfer, M. Saxinger, M. Schwegel, A. Steinboeck, and A. Kugi, "A two-stage observer for the compensation of actuator-induced disturbances in tool-force sensors", *Mechanical Systems and Signal Processing*, vol. 146, pp. 106989-1–106989-12, 2021, ISSN: 0888-3270. DOI: 10.1016/j.ymssp.2020.106989

can be used to improve the force measurements. If the behavior of the actuator changes over time, the actuator model has to be adapted. In this paper, a novel two-stage observer strategy for improving the measurement signal of the actuator force is developed. In this strategy, the time-varying characteristics of the tool and its measured input signal are systematically included. Furthermore, the disturbances in the measurement signal, which inevitably occur due to the placement of the sensor, are taken into account utilizing a suitable mechanical model in the second observer stage.

An example for a tool with a time-varying characteristics is a magnetic actuator where the magnetic properties of the handled workpiece may vary over time. For instance, magnetic actuators can be used for contactless transportation of steel plates [20]. If the magnetic force applied to the conveyed material is measured, the weight of the transported material or its magnetic properties can be determined. This can be valuable for production quality management. Furthermore, magnetic actuators are also employed in hot-dip galvanizing lines [21]. Here, a steel strip is elastically deformed and oscillations of the strip are damped [22]. If the magnetic force is measured, it can be used to determine shape errors of the metal strip, which is important for monitoring the product quality. Another area of application is the measurement of forces in active magnetic bearings. These bearings are used in applications, where high rotational speed and/or low bearing losses are demanded [23]. The force on the bearing can be exploited for monitoring the condition of the machine. Since correct measurement of magnetic forces has a broad field of applications, an experimental test rig with an electromagnetic actuator is set up to demonstrate the feasibility of the proposed two-stage observer strategy for the force measurement. It is worth noting that this strategy is not limited to the type of magnetic actuators.

The paper is organized as follows: The working principle of the electrical and mechanical part of a general sensor-actuator configuration is analyzed in Section 2. Furthermore, the source of actuator-induced disturbances, which deteriorate the measurements, is examined. Finally it is shown, how additional measurements can be used to compensate for the induced mechanical disturbances. In Section 3, an observer strategy is derived, which is able to suppress the actuator-induced disturbances without additional measurements. An experimental test rig, consisting of a magnetic actuator and a force sensor, is presented in Section 4. Experimental results obtained on this test rig using the developed two-stage observer strategy are also discussed in this section. The results are summarized in Section 5.

2. Measurement Principle and Actuator-Induced Disturbances

It is a common task to measure the force applied by an actuated tool to a workpiece. The tool can for instance be an end effector of a robotic arm or an actuator mounted on a fixed ground position. The tool is usually much heavier than the force sensor and thus, the mass of the sensor is neglected in the following. However, whenever the true tool force should be measured, it is in most cases not directly accessible to the force sensor. Either the tool (or parts of it) or the workpiece separates the position of the sensor from the position of the true tool force. Since force sensors always exhibit a certain compliance and damping behavior, a spring-mass-damper system emerges that disturbs the force measurement. In an ideal configuration, the force sensor is located between the workpiece and the plant, as shown in Fig. 1(a). Here, the force transferred by the sensor equals the tool force. A real configuration, in contrast, is shown in Fig. 1(b). Figure 1(c) shows another possibility where the force sensor is placed between the workpiece and the environment. This configuration suffers from the same disadvantages as for the one shown in Fig. 1(b), which is why it will not be discussed in more detail.

There exist a number of different force-sensing principles, e. g., sensors based on surface acoustic waves, magnetoelastic effects, vibrating wires or optic effects, cf. [24]. But almost all commercially available force sensors measure the force-induced strain in an elastic element by means of strain gauges, mainly because of its accuracy and simplicity. Thus, the force is indirectly measured by a displacement according to Hooke's law

$$F_\mathrm{s} = kz\,, \tag{1}$$

where F_s is the force measurement reading, k is the stiffness and z the deflection of the sensor [24]. As it will be seen, F_s may differ from the true force exerted on the sensor. If the sensor is placed as shown in Fig. 1(b), the combination of the force sensor and the tool can be described by a spring-mass-damper system as shown in Fig. 2. Here, the mass of the tool or the relevant parts of it is denoted by m and d is the viscous damping coefficient associated with the sensor, which is due to the energy dissipation in the sensor and its mounting. Based on Fig. 2, the tool force F_t and

Post-print version of the article: U. Knechtelsdorfer, M. Saxinger, M. Schwegel, A. Steinboeck, and A. Kugi, "A two-stage observer for the compensation of actuator-induced disturbances in tool-force sensors", *Mechanical Systems and Signal Processing*, vol. 146, pp. 106989-1–106989-12, 2021, ISSN: 0888-3270. DOI: 10.1016/j.ymssp.2020.106989
The content of this post-print version is identical to the published paper but without the publisher's final layout or copy editing.

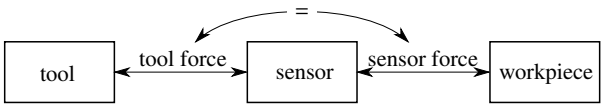

(a) Ideal configuration

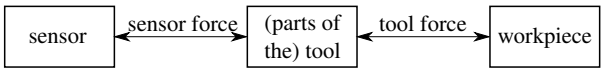

(b) Real configuration I

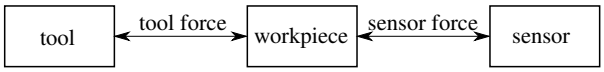

(c) Real configuration II

Figure 1: Configuration of a force sensor and a tool in (a) an ideal and (b and c) in a real force measurement setup.

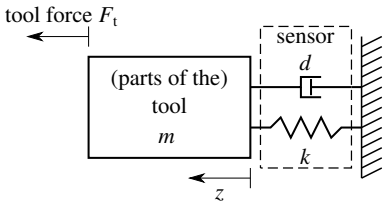

Figure 2: Combination of tool and force sensor.

the measurement reading F_s are related in the form

$$m\frac{\mathrm{d}^2 z}{\mathrm{d}t^2} + \underbrace{d\frac{\mathrm{d}z}{\mathrm{d}t} + F_\mathrm{s}}_{\substack{\text{force transferred}\\ \text{by the sensor}}} = F_\mathrm{t}\,. \tag{2}$$

Even if the sensor is not mounted on a rigid base as shown in Fig. 2, but on a flexible structure with a negligible mass, equation (2) is still applicable. In this case, d and k denote the effective stiffness and damping coefficient, respectively, of the combination of the sensor and its mounting. Clearly, if $\frac{\mathrm{d}^2 z}{\mathrm{d}t^2} \neq 0$ and $\frac{\mathrm{d}z}{\mathrm{d}t} \neq 0$, the measurement reading of the force sensor is disturbed by the inertia and damping forces, respectively. As an example, Fig. 3 shows measurement results of a laboratory experiment. In this experiment, a ferromagnetic workpiece is loaded with a piecewise constant force applied by an electromagnetic actuator. Some key parameters of the utilized equipment can be found in Tab. 1. The true tool force F_t (pink) can be determined from the steady-state response of the measurement reading. The gray line represents the measurement reading of the force sensor, i. e., F_s in (2). The measurement results show that large oscillations with the natural frequency are contained in the measured signal. In the considered setup, the natural frequency is about 47 Hz. This systematic measurement error is caused by the first two terms in (2) and can be eliminated or at least reduced by using additional sensors, by measuring the acceleration or the position of the tool.

First, let us assume that the position z is known with a sufficiently high accuracy. In the considered experimental test rig, this is achieved by a laser interferometer. This assumption is in most practical cases infeasible and will thus not be considered in the upcoming sections, but is assumed only here to analyze the potential of compensating the inertia and damping forces in the measurement reading. Based on the position information $z(t)$, the velocity and the

Post-print version of the article: U. Knechtelsdorfer, M. Saxinger, M. Schwegel, A. Steinboeck, and A. Kugi, "A two-stage observer for the compensation of actuator-induced disturbances in tool-force sensors", *Mechanical Systems and Signal Processing*, vol. 146, pp. 106989-1–106989-12, 2021, ISSN: 0888-3270. DOI: 10.1016/j.ymssp.2020.106989

Table 1: Experiment specification data.

Force sensor:	Inelta KMM30	
	Force range	0 – 500N
	Resolution	10 mN
	Frequency range	0 – 900Hz
Laser interferometer:	Polytec OFV-5000	
	Position range	±1000 µm
	Resolution	30 nm
	Frequency range	0 – 250kHz
Acceleration sensor:	Kistler 5165A4 / 8640A50T	
	Acceleration range	500 m s^{-2}
	Resolution	10 mm s^{-2}
	Frequency range	0.5 – 3000Hz
Magnetic tool:	custom made	
	Tool mass	9 kg
	Control input range	±15 A
	Number of windings	280

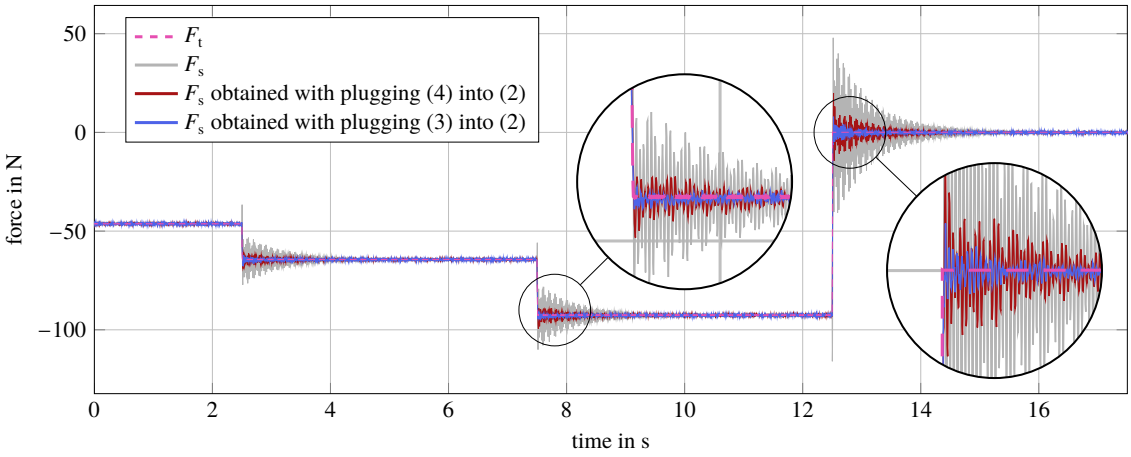

Figure 3: Raw force signal and force signal with compensated mechanical oscillation.

acceleration can be approximated by the difference quotients

$$\frac{\mathrm{d}}{\mathrm{d}t}z(t) \approx \frac{z(t) - z(t-\Delta t)}{\Delta t} \tag{3a}$$

$$\frac{\mathrm{d}^2}{\mathrm{d}t^2}z(t) \approx \frac{z(t) - 2z(t-\Delta t) + z(t-2\Delta t)}{\Delta t^2}, \tag{3b}$$

with an appropriately chosen time step Δt. Here, Δt is chosen as $\Delta t = 1/f_s$, where $f_s = 1\,\mathrm{kHz}$ is the sampling frequency at which the measurement is recorded. The blue line in Fig. 3 represents (the time evolution of) F_t based on (2) with $\frac{\mathrm{d}^2 z}{\mathrm{d}t^2}$ and $\frac{\mathrm{d}z}{\mathrm{d}t}$ from (3). The disturbances due to the mechanical oscillations are suppressed, as the results in Fig. 3 show. The remaining error in the compensated force signal can be attributed to measurement noise in the position signal, which is amplified due to the second order derivative. Still, the correction of the force measurement based on the position measured by the laser interferometer is performing well.

Another possibility is to assume that the acceleration of the tool

$$a = \frac{\mathrm{d}^2}{\mathrm{d}t^2}z(t) \tag{4a}$$

can be measured by an acceleration sensor. Most acceleration sensors which are used in industrial environments

Post-print version of the article: U. Knechtelsdorfer, M. Saxinger, M. Schwegel, A. Steinboeck, and A. Kugi, "A two-stage observer for the compensation of actuator-induced disturbances in tool-force sensors", *Mechanical Systems and Signal Processing*, vol. 146, pp. 106989-1–106989-12, 2021, ISSN: 0888-3270. DOI: 10.1016/j.ymssp.2020.106989

are based on the piezoelectric effect. These sensors are known to be prone to disturbances, especially in the low frequency range, see, e. g., [25]. Thus, the measured acceleration signal needs to be high-pass filtered before it can be used for compensation of the mechanical disturbances in the measured force signal. The velocity of the tool can be approximated by integration of the acceleration signal a, e. g., with Euler's method

$$\frac{\mathrm{d}}{\mathrm{d}\,t} z(t) \approx \sum_{\{\forall n | n\Delta t < t,\, n \in \mathbb{N}\}} a(n\Delta t)\Delta t\,. \tag{4b}$$

Inserting (4) into (2) again leads to a suppression of the disturbances in the measured force signal. Figure 3 shows the measured force signal compensated with the measured acceleration signal as red line. Compared to the previous compensation method, using the acceleration sensors leads to a larger remaining error. This error is due to a time delay caused by the pre-amplifier of the measurement signal.

In conclusion, it was shown in this section that the measured force signal can be corrected by measurements of the mechanical movements of the tool. Since additional sensors always entail higher costs and more effort in construction and assembling, a compensation strategy solely based on the already existing measurements will be developed in the next section.

3. Two-Stage Observer

In the following, a two-stage observer strategy will be developed for the tool force F_t. It is assumed that the tool force F_t is the sum of a known static component $F_\mathrm{t,e}$ (stage 1), which describes the steady-state input-output characteristics between the control input u and the tool force, and a generally unknown component ΔF_t (stage 2), which has to be estimated, i.e.,

$$F_\mathrm{t} = F_\mathrm{t,e} + \Delta F_\mathrm{t}\,. \tag{5}$$

For the first stage, it is assumed that the known static input-output characteristics from the control input u to the tool force $F_\mathrm{t,e}$ can be approximated in the form

$$F_\mathrm{t,e} = \sum_{n=0}^{N} u^n a_n = \mathbf{u}^\mathrm{T}\mathbf{a}\,, \tag{6}$$

where the polynomial coefficients and the control input can be expressed as vectors $\mathbf{a} = \begin{bmatrix} a_0 & a_1 & \dots & a_N \end{bmatrix}^\mathrm{T}$ and $\mathbf{u} = \begin{bmatrix} 1 & u^1 & \dots & u^N \end{bmatrix}^\mathrm{T}$, respectively. The control input u is the coil current of the electromagnetic actuator considered in this work, but it may also be another quantity like the valve opening of a pneumatic actuator or the voltage of an electrostatic actuator. Using the steady-state input-output model (6) can be justified if the transient response of the actuator decays much faster than the transient response of the spring-mass-damper system according to Fig. 2. If this requirement is not fulfilled, a dynamic model has to be used instead of (6). The coefficients $\mathbf{a}$ can be identified based on a dedicated measurement campaign. Due to the different materials of the workpieces, an a-priori identification is not always feasible and its results would not be valid for a long period. Such differences and variations of material properties are further examined in Section 4. Thus, the coefficients $\mathbf{a}$ are estimated online by a recursive least-squares algorithm with exponential forgetting according to [26]. For this purpose, the integrated quadratic error

$$\min_{\mathbf{a}(t)} \frac{1}{2} \int_0^t \exp\left(\gamma(\tau - t)\right) \left(F_\mathrm{s}(\tau) - \mathbf{u}^\mathrm{T}(\tau)\mathbf{a}(t)\right)^2 \mathrm{d}\,\tau\,, \tag{7}$$

between the force measurement reading F_s and the force estimate due to the control input is minimized. In (7), $\exp\left(\gamma\left(\tau - t\right)\right)$ is a weighting factor and $\gamma \geq 0$ denotes the forgetting factor. From the first-order optimality condition,

Post-print version of the article: U. Knechtelsdorfer, M. Saxinger, M. Schwegel, A. Steinboeck, and A. Kugi, "A two-stage observer for the compensation of actuator-induced disturbances in tool-force sensors", *Mechanical Systems and Signal Processing*, vol. 146, pp. 106989-1–106989-12, 2021, ISSN: 0888-3270. DOI: 10.1016/j.ymssp.2020.106989
The content of this post-print version is identical to the published paper but without the publisher's final layout or copy editing.

it follows that [26]

$$\underbrace{\int_0^t \exp\left(\gamma(\tau - t)\right) \mathbf{u}(\tau)\mathbf{u}^{\mathrm{T}}(\tau)\,\mathrm{d}\,\tau}_{=\mathbf{P}}\ \mathbf{a} = \mathbf{P}\mathbf{a} = \int_0^t \exp\left(\gamma(\tau - t)\right) \mathbf{u}(\tau) F_{\mathrm{s}}(\tau)\,\mathrm{d}\,\tau\,. \tag{8}$$

Using the identity

$$\frac{\mathrm{d}}{\mathrm{d}\,t}\mathbf{P} = -\gamma\mathbf{P} + \mathbf{u}\mathbf{u}^{\mathrm{T}}\,, \quad \mathbf{P}(0) = \mathbf{P}_0\,, \tag{9}$$

in the time derivative of (8) gives

$$\left(\frac{\mathrm{d}}{\mathrm{d}\,t}\mathbf{P}\right)\mathbf{a} + \mathbf{P}\left(\frac{\mathrm{d}}{\mathrm{d}\,t}\mathbf{a}\right) = -\gamma\mathbf{P}\mathbf{a} + \mathbf{u}\mathbf{u}^{\mathrm{T}}\mathbf{a} + \mathbf{P}\left(\frac{\mathrm{d}}{\mathrm{d}\,t}\mathbf{a}\right) = -\gamma \underbrace{\int_0^t \exp\left(\gamma(\tau - t)\right) \mathbf{u}(\tau) F_{\mathrm{s}}(\tau)\,\mathrm{d}\,\tau}_{=\mathbf{P}\mathbf{a}} + \mathbf{u}F_{\mathrm{s}}\,. \tag{10}$$

This yields the update law

$$\frac{\mathrm{d}}{\mathrm{d}\,t}\mathbf{a} = \mathbf{P}^{-1}\mathbf{u}\left(F_{\mathrm{s}} - \mathbf{u}^{\mathrm{T}}\mathbf{a}\right)\,, \quad \mathbf{a}(0) = \mathbf{a}_0 \tag{11}$$

for the estimated parameters $\mathbf{a}$. For a time $t > 0$ the matrix $\mathbf{P}$ and the estimated parameters $\mathbf{a}$ can be computed by integration of (9) and (11). The computationally expensive inversion of $\mathbf{P}$ can be omitted by direct integration of $\frac{\mathrm{d}}{\mathrm{d}\,t}\mathbf{P}^{-1}$. In fact, insertion of (9) into

$$\left(\frac{\mathrm{d}}{\mathrm{d}\,t}\mathbf{P}\mathbf{P}^{-1}\right) = \mathbf{0} = \left(\frac{\mathrm{d}}{\mathrm{d}\,t}\mathbf{P}\right)\mathbf{P}^{-1} + \mathbf{P}\left(\frac{\mathrm{d}}{\mathrm{d}\,t}\mathbf{P}^{-1}\right) \tag{12}$$

yields

$$\frac{\mathrm{d}}{\mathrm{d}\,t}\mathbf{P}^{-1} = \gamma\mathbf{P}^{-1} - \mathbf{P}^{-1}\mathbf{u}\mathbf{u}^{\mathrm{T}}\mathbf{P}^{-1}\,, \quad \mathbf{P}^{-1}(0) = \mathbf{P}_0^{-1}\,. \tag{13}$$

The nominal parameters of the tool model (6) serve as initial parameters $\mathbf{a}_0$. In order to ensure a good convergence behavior, the matrix $\mathbf{P}_0$ is chosen as $\mathbf{P}_0 = p_0\mathbf{I}$, with the identity matrix $\mathbf{I}$ and a sufficiently small positive parameter p_0.

For the second stage, a reduced Luenberger observer is designed, for the theory, see, e. g., [27]. It systematically takes into account the mass-spring-damper system resulting from the sensor configuration according to Fig. 2. For the observer design, it is assumed that the unknown component of the tool force ΔF_{t} is constant, i.e. $\frac{\mathrm{d}}{\mathrm{d}\,t}\Delta F_{\mathrm{t}} = 0$. Combining the disturbance model for ΔF_{t} with (2) and (5) yields

$$\frac{\mathrm{d}}{\mathrm{d}\,t}\begin{bmatrix} kz \\ v \\ \Delta F_{\mathrm{t}} \end{bmatrix} = \begin{bmatrix} 0 & k & 0 \\ -\frac{1}{m} & -\frac{d}{m} & \frac{1}{m} \\ 0 & 0 & 0 \end{bmatrix}\begin{bmatrix} kz \\ v \\ \Delta F_{\mathrm{t}} \end{bmatrix} + \begin{bmatrix} 0 \\ \frac{1}{m} \\ 0 \end{bmatrix} F_{\mathrm{t,e}} \tag{14a}$$

$$F_{\mathrm{s}} = \begin{bmatrix} 1 & 0 & 0 \end{bmatrix}\begin{bmatrix} kz \\ v \\ \Delta F_{\mathrm{t}} \end{bmatrix}, \tag{14b}$$

with $v = \frac{\mathrm{d}}{\mathrm{d}\,t}z$. Equation (14b) indicates that the first state $F_{\mathrm{s}} = kz$ can be directly measured, cf. (1). This means that (14a) is formulated in sensor coordinates. For the measured state $F_{\mathrm{s}} = kz$ and for the unmeasured states $\mathbf{x} = \begin{bmatrix} v & \Delta F_{\mathrm{t}} \end{bmatrix}^{\mathrm{T}}$, the dynamics can be written as

$$\frac{\mathrm{d}}{\mathrm{d}\,t}F_{\mathrm{s}} = \mathbf{F}\mathbf{x}\,, \quad \mathbf{F} = \begin{bmatrix} k & 0 \end{bmatrix} \tag{15}$$

Post-print version of the article: U. Knechtelsdorfer, M. Saxinger, M. Schwegel, A. Steinboeck, and A. Kugi, "A two-stage observer for the compensation of actuator-induced disturbances in tool-force sensors", *Mechanical Systems and Signal Processing*, vol. 146, pp. 106989-1–106989-12, 2021, ISSN: 0888-3270. DOI: 10.1016/j.ymssp.2020.106989
The content of this post-print version is identical to the published paper but without the publisher's final layout or copy editing.

and

$$\frac{\mathrm{d}}{\mathrm{d}t}\mathbf{x} = \mathbf{A}\mathbf{x} + \mathbf{B}\left(F_\mathrm{s} - F_\mathrm{t,e}\right) , \tag{16}$$

with

$$\mathbf{A} = \begin{bmatrix} -\frac{d}{m} & \frac{1}{m} \\ 0 & 0 \end{bmatrix} \quad \text{and} \quad \mathbf{B} = \begin{bmatrix} -\frac{1}{m} \\ 0 \end{bmatrix} . \tag{17}$$

For the dynamic system (16), there does not exist a measurable output. However, an output according to (15) can be defined. If this output is used for an observer design, the time derivative $\frac{\mathrm{d}}{\mathrm{d}t}F_\mathrm{s}$ of the force measurement reading is required. Differentiation of measured variables is undesirable because of measurement noise. Thus, as suggested in [27], a state transformation

$$\mathbf{w} = \mathbf{x} - \mathbf{L}F_\mathrm{s} , \tag{18}$$

with a constant vector $\mathbf{L} \in \mathbb{R}^2$, is introduced. With this transformation and the relation (15), the dynamic model

$$\frac{\mathrm{d}}{\mathrm{d}t}\mathbf{w} = \left(\mathbf{A} - \mathbf{L}\mathbf{F}\right)\left(\mathbf{w} + \mathbf{L}F_\mathrm{s}\right) + \mathbf{B}\left(F_\mathrm{s} - F_\mathrm{t,e}\right) \tag{19}$$

is obtained. A trivial observer for the transformed state $\mathbf{w}$ reads as

$$\frac{\mathrm{d}}{\mathrm{d}t}\hat{\mathbf{w}} = \left(\mathbf{A} - \mathbf{L}\mathbf{F}\right)\left(\hat{\mathbf{w}} + \mathbf{L}F_\mathrm{s}\right) + \mathbf{B}\left(F_\mathrm{s} - F_\mathrm{t,e}\right) . \tag{20}$$

With the observer error

$$\hat{\mathbf{e}} = \hat{\mathbf{w}} - \mathbf{w} , \tag{21}$$

the error dynamics takes the form

$$\frac{\mathrm{d}}{\mathrm{d}t}\hat{\mathbf{e}} = \left(\mathbf{A} - \mathbf{L}\mathbf{F}\right)\hat{\mathbf{e}} . \tag{22}$$

By choosing $\mathbf{L}$, the observer error dynamics (22) can be arbitrarily defined because the pair $(\mathbf{F}, \mathbf{A})$ is observable. In any case, the observer dynamics should be slower than the natural frequency of the mass-spring-damper system to ensure the assumption of a constant disturbance is valid. As it is desired to directly specify the dynamics of (22), pole placement is the first choice. Thus, $\mathbf{L}$ can be computed by Ackermann's pole-placement formula. Note that in principle, it would be also possible to use a reduced-order Kalman filter, see, e. g., [28], but this does not have any advantages in the considered application. Instead of employing a reduced-order Luenberger observer for (16), a full state observer could be designed for the system (14). However, since the sensor reading F_s features low noise, the selection was made for the reduced-order Luenberger observer because it is simpler and easier to tune.

Finally, the estimated value of the unknown tool force component can be computed in the form, (see (18)),

$$\Delta\hat{F}_\mathrm{t} = \begin{bmatrix} 0 & 1 \end{bmatrix}\left(\hat{\mathbf{w}} + \mathbf{L}F_\mathrm{s}\right) . \tag{23}$$

If the reduced Luenberger observer for ΔF_t is combined with the static estimation $F_\mathrm{t,e}$ of the tool force according to the steady-state tool model, an estimation of the total tool force

$$\hat{F}_\mathrm{t} = F_\mathrm{t,e} + \Delta\hat{F}_\mathrm{t} \tag{24}$$

is obtained. The structure of the two-stage observer, including the online recursive least-squares estimation (LSQ) of the steady-state tool characteristics and the reduced Luenberger observer, is shown in Fig. 4.

In contrast to [13], the estimated parameters are not directly utilized in the model of the second stage. Thus, the

Post-print version of the article: U. Knechtelsdorfer, M. Saxinger, M. Schwegel, A. Steinboeck, and A. Kugi, "A two-stage observer for the compensation of actuator-induced disturbances in tool-force sensors", *Mechanical Systems and Signal Processing*, vol. 146, pp. 106989-1–106989-12, 2021, ISSN: 0888-3270. DOI: 10.1016/j.ymssp.2020.106989
The content of this post-print version is identical to the published paper but without the publisher's final layout or copy editing.

second stage is a linear time invariant (LTI) system, where stability of the estimation error is readily ensured by proper choice of **L**, cf., (22). Exponential convergence of the estimation in the first stage of the observer is ensured under the premise of a persistent excitation.

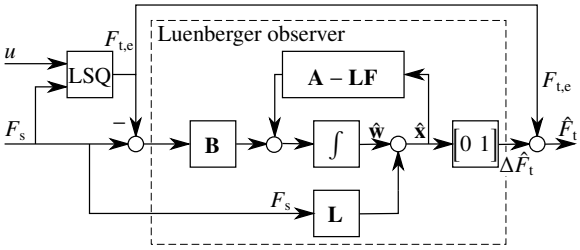

Figure 4: Two-stage observer structure.

4. Experimental Setup and Measurement Results

To demonstrate the suitability of the proposed two-stage observer strategy, an experimental test rig was developed, see, Fig. 5. The essential parts of the experimental setup are highlighted in the photo Fig. 5(a). In this setup, the tool is an electromagnetic actuator. However, the proposed observer strategy is not limited to this configuration. The electromagnetic actuator applies a force to a spatially fixed workpiece consisting of ferromagnetic material. It is assumed that the coil current serves as control input u, which is realized by a fast subordinate current control loop. Thus, the electromagnetic force can be considered as a nonlinear function of the coil current u, the magnetic properties of the material and the distance (air gap) between the electromagnetic actuator and the workpiece, which, apart from vibrations, is nearly constant in the considered case. The parallelogram structure holding the electromagnetic actuator

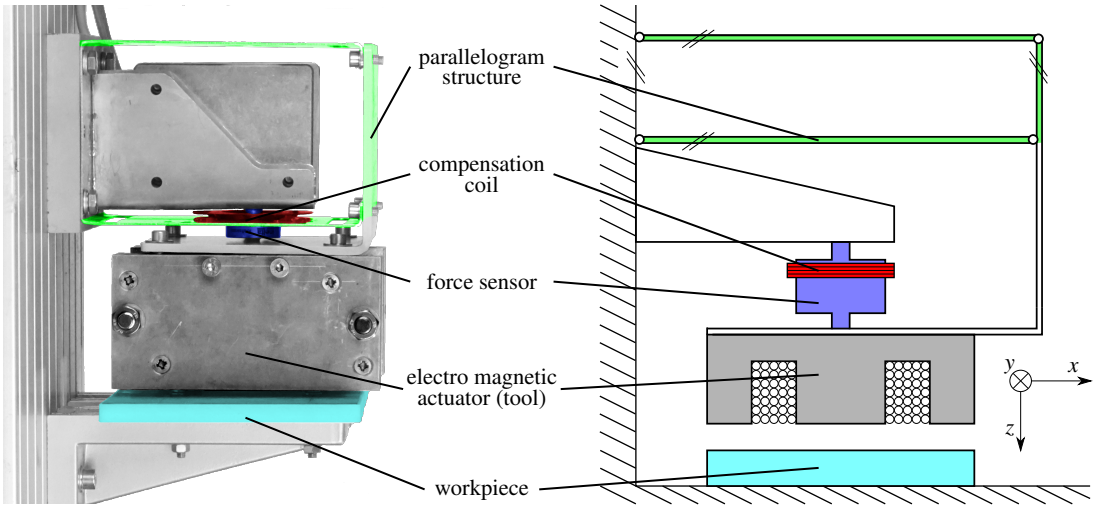

(a) Photo of the experiment.

(b) Schematic representation of the experiment.

Figure 5: Experimental test rig with electromagnetic actuator, workpiece and integrated force sensor.

in place, see, Fig. 5, results in a high deformation stiffness in y- and x-direction but low stiffness in z-direction. Furthermore, this design inhibits rotational movements of the electromagnetic actuator. Thus, force on the force sensor can only be applied along the z-direction. Hence, the experimental test rig can be represented by the equivalent model according to Fig. 2. Note that this experimental test rig serves as a laboratory model for the actuators used in hot-dip galvanizing lines to stabilize the transverse displacement of a moving metal strip, see, e. g., [21, 22].

Post-print version of the article: U. Knechtelsdorfer, M. Saxinger, M. Schwegel, A. Steinboeck, and A. Kugi, "A two-stage observer for the compensation of actuator-induced disturbances in tool-force sensors", *Mechanical Systems and Signal Processing*, vol. 146, pp. 106989-1–106989-12, 2021, ISSN: 0888-3270. DOI: 10.1016/j.ymssp.2020.106989

The electromagnetic actuator induces magnetic stray flux which may also disturb the force sensor. Due to space and weight limitations, it is not possible to overcome this issue by redesigning the magnet holder. Therefore, a method will be presented which allows to compensate for the stray flux induced disturbances in the force measurement signal. The force sensor measures the force indirectly by strain gauges in the sensor housing. The strain gauges form a resistive bridge circuit, which allows the conversion of the strain value into an electric voltage. This is then amplified by a factor β and the output of the amplifier represents the force measurement reading F_s. Unfortunately, conventional

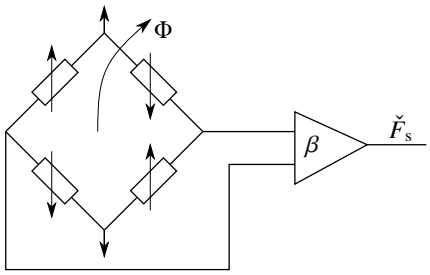

Figure 6: Induced disturbances due to changing magnetic flux.

force sensors are generally not shielded against magnetic fluxes. If a time-varying magnetic flux Φ flows through the strain gauge bridge as outlined in Fig. 6, a voltage v_s proportional to the change of the flux is induced according to Faraday's law of induction [29]. Thus, the measurement reading of the force sensor

$$\check{F}_\mathrm{s} = F_\mathrm{s} + \beta v_\mathrm{s} \tag{25}$$

is disturbed by the magnetically induced voltage v_s. In order to measure and compensate for the disturbances caused by the induced voltage, an additional coil is placed in the vicinity of the force sensor. In this coil, a voltage v_c is induced. The relation between v_s and v_c is given in the form

$$\frac{v_\mathrm{s}}{v_\mathrm{c}} = \frac{A_\mathrm{s}}{A_\mathrm{c} N_\mathrm{c}}\,, \tag{26}$$

where A_s is the area spanned by the strain gauge bridge, A_c is the area of the coil, and N_c is its number of windings. Here, it is assumed that the magnetic flux in the vicinity of the force sensor is homogeneous. The sensor reading can thus be corrected by the compensation law

$$F_\mathrm{s} = \check{F}_\mathrm{s} - \underbrace{\beta \frac{A_\mathrm{s}}{A_\mathrm{c} N_\mathrm{c}}}_{\beta_\mathrm{c}} v_\mathrm{c}\,, \tag{27}$$

where all the constants can be combined to one factor β_c. Because A_s is effectively unknown, β_c has to be identified, which can easily be done by subjecting the unloaded force sensor to a varying magnetic field. In this case, the expected force measurement F_s is 0 N. Therefore, the sensor reading $\check{F}_\mathrm{s}$ shows only the magnetically induced disturbance, cf. (25). The factor β_c can thus be identified by minimizing the quadratic cost function

$$\min_{\beta_\mathrm{c}} \int_0^T \left(\check{F}_\mathrm{s}(\tau) - \beta_\mathrm{c} v_\mathrm{c}(\tau)\right)^2 \mathrm{d}\,\tau \tag{28}$$

where T is the duration of the calibration measurement. A measurement campaign demonstrating the feasibility of the compensation of magnetic disturbances is shown in Fig. 7. Here, the workpiece is removed, so the expected force reading is 0 N. The control input of the electromagnetic actuator is a sinusoidal coil current with various frequencies. These frequencies are also indicated in Fig. 7. The sensor noise level can be inferred from the section corresponding to 0 Hz. The compensated force measurement signal according to (27) is within the boundaries of the sensor noise level for low frequencies of the coil current. For frequencies > 15 Hz, the remaining disturbance increases but is still

Post-print version of the article: U. Knechtelsdorfer, M. Saxinger, M. Schwegel, A. Steinboeck, and A. Kugi, "A two-stage observer for the compensation of actuator-induced disturbances in tool-force sensors", *Mechanical Systems and Signal Processing*, vol. 146, pp. 106989-1–106989-12, 2021, ISSN: 0888-3270. DOI: 10.1016/j.ymssp.2020.106989
The content of this post-print version is identical to the published paper but without the publisher's final layout or copy editing.

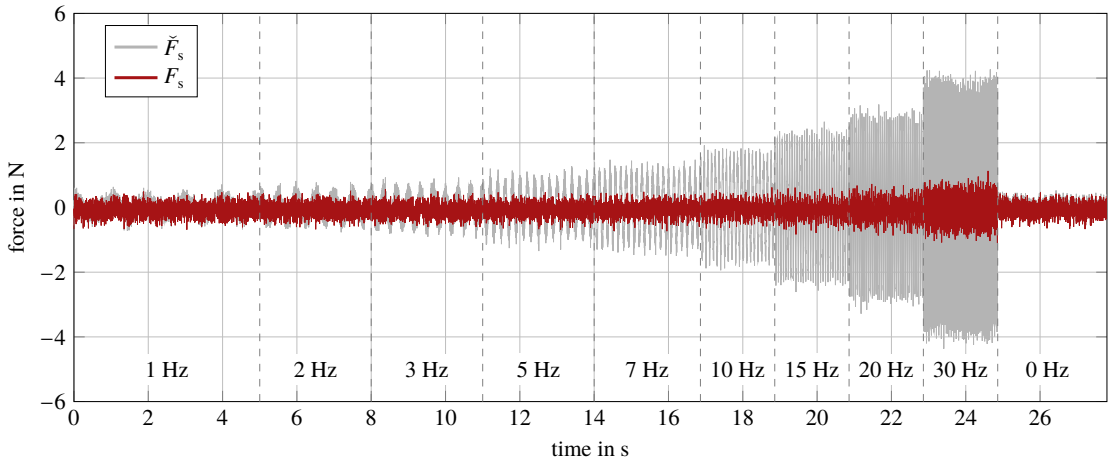

Figure 7: Force sensor reading and force signal with compensated disturbances due to the magnetic stray fluxes

significantly lower than the measurement error without compensation.

An experiment similar to the one presented in Fig. 3 is performed to demonstrate the feasibility of the proposed two-stage observer strategy. A piecewise constant input current is applied to the electromagnetic actuator. Hence, a piecewise constant tool force can be expected. In this experiment, the eigenvalues of the observer error dynamics, cf. (22), are chosen as $-50\,\mathrm{s}^{-1}$ and $-60\,\mathrm{s}^{-1}$, which are slower than the natural frequency of the tool-sensor combination. The results are shown in Fig. 8. The force sensor reading (gray) is compared to the estimated force signal according to the observer structure of Fig. 4 (red) and to the estimated force signal which is obtained by the observer alone, i. e., when setting $F_{\mathrm{t,e}} = 0$ (blue) in (5). In both cases, the disturbances in the measurement signal can be very well suppressed. Moreover, Fig. 8 shows that the tool force can be estimated without a steady-state error. According to the detail views of Fig. 8, the two-stage observer strategy comprising the least-squares estimation of the static input-output characteristics $F_{\mathrm{t,e}}$ exhibits a faster response to changes of the control input because the first stage systematically exploits the information due to the changing tool actuation.

Another measurement campaign, shown in Fig. 9, mimics a scenario in a control application. Here, the electromagnetic actuator is excited with a sinusoidal control input (10 Hz) with a constant offset. This scenario is typical, e. g. if the electromagnetic actuator is used for strip stabilization in a hot-dip galvanizing line [22]. The area labeled ① shows a nominal scenario. In the laboratory environment, the true tool force F_{t} can be determined by a lookup table which maps the values of the control input u to the corresponding steady-state tool force. The lookup table must be generated in an additional measurement campaign.

The observed signal which is obtained by the observer alone, i. e., when setting $F_{\mathrm{t,e}} = 0$, shows a significantly damped amplitude and a phase shift, which can be seen in the detail view of Fig. 9. In contrast, the proposed observer structure, which exploits the known actuation of the tool, is in good accordance with the true tool force. For the sake of comparison, an observer with the structure shown in Fig. 4 but a static a-priori identification of the tool force (6) is employed. Figure. 9 shows that the static approximation of the tool force performs similar to the online least-squares identification of the tool force in the area labeled ①.

Although hot-dip galvanizing is a continuous process, a sharp change between the magnetic properties of the processed strip occurs frequently. This is because the processed endless strip consists of single strips which are welded together and thus lead to piecewise constant material parameters, which influence the static input-output characteristics of the tool. In the area labeled ②, a change of the strip parameters is emulated. In the area labeled ③, the parameters of the workpiece are held constant again. At the beginning of the area labeled ③, there is a notable measurement error between F_{t} and the observed force $\hat{F}_{\mathrm{t}}$. However, as soon as the estimated tool model (6) adapts, the estimation error in amplitude and force converges to zero. This is not the case, if the tool characteristics are identified in advance offline. Thus, it is shown that the developed two-stage observer with an online estimation of the static input-output characteristics is also superior to an offline identification.

Post-print version of the article: U. Knechtelsdorfer, M. Saxinger, M. Schwegel, A. Steinboeck, and A. Kugi, "A two-stage observer for the compensation of actuator-induced disturbances in tool-force sensors", *Mechanical Systems and Signal Processing*, vol. 146, pp. 106989-1–106989-12, 2021, ISSN: 0888-3270. DOI: 10.1016/j.ymssp.2020.106989
The content of this post-print version is identical to the published paper but without the publisher's final layout or copy editing.

As shown in the detail view of Fig. 9, the resulting force is nearly sinusoidal. Therefore, Fig. 10 shows the amplitude and phase error of the first harmonics between $\hat{F}_\mathrm{t}$ and F_t. After the strip parameters are changed, the phase and amplitude error between $\hat{F}_\mathrm{t}$ and F_t converge to negligibly low values in the case of online estimation of the coefficients a_n. In contrast, if the estimation of the parameters a_n is done in advance, errors in the amplitude and phase remain.

Furthermore, Fig. 10 shows the amplitude and phase error between $F_\mathrm{t,e}$ and F_t. Taking $\hat{F}_\mathrm{t} = F_\mathrm{t,e}$ as estimation of F_t equals the observer structure shown in Fig. 4 with $\Delta F_\mathrm{t} = 0$, meaning that the tool force is estimated only by the least-squares algorithm. In this case, even if the amplitude error decays, an error in the phase remains. This demonstrates that the proposed two-stage observer structure is also superior to a pure least-squares estimation of the tool characteristics without consideration of the dynamical effects (i. e., $\Delta F_\mathrm{t} = 0$).

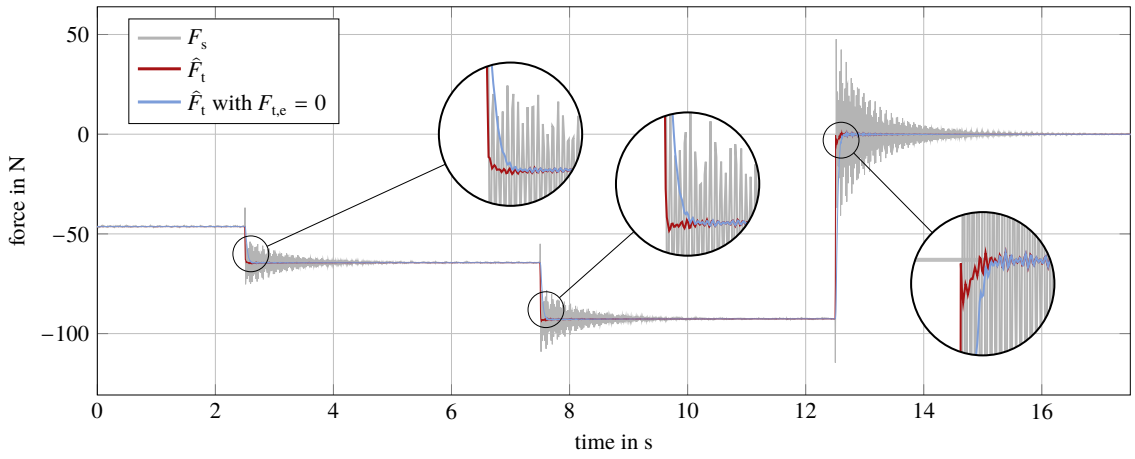

Figure 8: Force sensor reading and estimated force signal obtained by the observer introduced in Sec. 3: Step-like changes of the tool force.

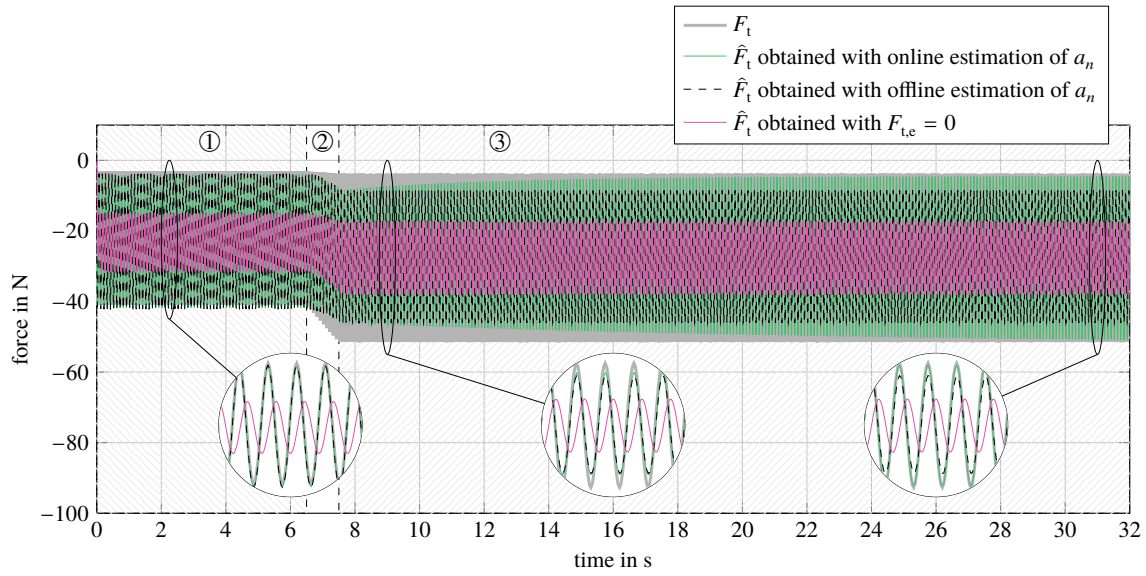

Figure 9: Force measurement reading and estimated force signal obtained by the observer introduced in Sec. 3: Sinusoidal changes of the tool force.

Post-print version of the article: U. Knechtelsdorfer, M. Saxinger, M. Schwegel, A. Steinboeck, and A. Kugi, "A two-stage observer for the compensation of actuator-induced disturbances in tool-force sensors", *Mechanical Systems and Signal Processing*, vol. 146, pp. 106989-1–106989-12, 2021, ISSN: 0888-3270. DOI: 10.1016/j.ymssp.2020.106989

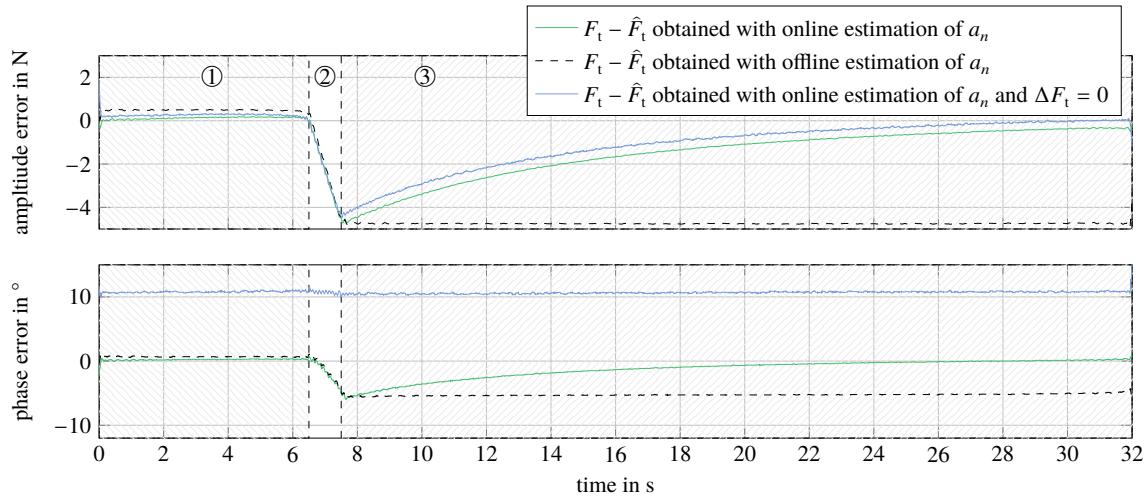

Figure 10: Phase and amplitude error of the first harmonics of the signals in Fig. 9.

5. Conclusions

This paper proposes a novel two-stage observer strategy for improving the measurement of tool forces by rejecting unwanted disturbances. In Section 1, a brief overview of already existing methods for compensating mechanical oscillations in the context of force measurements is given. Furthermore, potential areas of application of the proposed observer strategy are discussed. In Section 2, it is analyzed why mechanical oscillations can disturb the measurement of the tool forces and a simple dynamical model is derived. It is shown that the disturbances of the tool force measurement can be compensated by additional position or acceleration measurements. In Section 3, a two-stage observer strategy which is able to reject these disturbances without additional measurements is developed. The proposed observer consists of a recursive least-squares estimation of the input-output characteristics of the tool and a reduced Luenberger observer. The least-squares estimation of the tool force characteristics tracks fast changes of the tool force caused by the system input. The influence of the mechanical setup of the sensor-tool configuration, in contrast, is captured by the reduced Luenberger observer which also estimates the acceleration forces. This leads to an overall observer strategy which

- does not use additional sensors except for the existing force sensor,
- can reject the influence of inertia forces on the measurement signal, and
- responds quickly to changes of the input of the actuator.

The efficacy of the developed observer strategy was tested on a laboratory experiment, which is explained in Section 4. Additional disturbances induced by the stray fluxes of the magnetic actuator used in this experimental setup were analyzed and a method was proposed for their compensation. The obtained measurement results prove the feasibility of the proposed two-stage observer strategy.

6. Acknowledgements

The financial support by the Christian Doppler Research Association, the Austrian Federal Ministry for Digital and Economic Affairs, and the National Foundation for Research, Technology and Development is gratefully acknowledged. Special thanks are dedicated to Andreas Ettl for his contribution to the mechanical design of the laboratory experiment.

[1] Y. Fujii, Method for correcting the effect of the inertial mass on dynamic force measurements, Measurement Science and Technology 18 (5) (2007) N13–N20.

Post-print version of the article: U. Knechtelsdorfer, M. Saxinger, M. Schwegel, A. Steinboeck, and A. Kugi, "A two-stage observer for the compensation of actuator-induced disturbances in tool-force sensors", *Mechanical Systems and Signal Processing*, vol. 146, pp. 106989-1–106989-12, 2021, ISSN: 0888-3270. DOI: 10.1016/j.ymssp.2020.106989
The content of this post-print version is identical to the published paper but without the publisher's final layout or copy editing.

[2] S. S. Park, Y. Altintas, Dynamic compensation of spindle integrated force sensors with Kalman filter, Journal of Dynamic Systems, Measurement, and Control 126 (3) (2004) 443–452.
[3] A. Scippa, L. Sallese, N. Grossi, G. Campatelli, Improved dynamic compensation for accurate cutting force measurements in milling applications, Mechanical Systems and Signal Processing 54-55 (2015) 314 – 324.
[4] M. Wan, W. Yin, W.-H. Zhang, H. Liu, Improved inverse filter for the correction of distorted measured cutting forces, International Journal of Mechanical Sciences 120 (2017) 276–285.
[5] K. Kiran, M. C. Kayacan, Cutting force modeling and accurate measurement in milling of flexible workpieces, Mechanical Systems and Signal Processing 133 (2019) 106284–106305.
[6] D. Aslan, Y. Altintas, Prediction of cutting forces in five-axis milling using feed drive current measurements, IEEE/ASME Transactions on Mechatronics 23 (2) (2018) 833–844.
[7] M. Uchiyama, K. Kitagaki, Dynamic force sensing for high-speed robot manipulation using kalman filtering techniques, in: Proceedings of the 28th IEEE Conference on Decision and Control, Vol. 3, Tampa, Florida, USA, 1989, pp. 2147–2152.
[8] J. Garcia, A. Robertsson, J. Ortega, R. Johansson, Sensor fusion for compliant robot motion control, IEEE Transactions on Robotics 24 (2) (2008) 430–441.
[9] W. Shi, N. White, J. Brignell, Adaptive filters in load cell response correction, Sensors and Actuators A: Physical 37-38 (1993) 280–285.
[10] J. Piskorowski, T. Barcinski, Dynamic compensation of load cell response: A time-varying approach, Mechanical Systems and Signal Processing 22 (7) (2008) 1694–1704.
[11] V. Nguyen, S. N. Melkote, Modeling of flange-mounted force sensor frequency response function for inverse filtering of forces in robotic milling, Procedia Manufacturing 34 (2019) 804–812.
[12] K. Ohnishi, M. Shibata, T. Murakami, Motion control for advanced mechatronics, IEEE/ASME Transactions on Mechatronics 1 (1) (1996) 56–67.
[13] E. Sariyildiz, K. Ohnishi, An adaptive reaction force observer design, IEEE/ASME Transactions on Mechatronics 20 (2) (2015) 750–760.
[14] G. Garofalo, N. Mansfeld, J. Jankowski, C. Ott, Sliding mode momentum observers for estimation of external torques and joint acceleration, in: Proceedings of 2019 International Conference on Robotics and Automation (ICRA), IEEE, 2019, pp. 6117–6123.
[15] R. Osypiuk, J. Piskorowski, D. Kubus, A method of improving the dynamic response of 3D force/torque sensors, Mechanical Systems and Signal Processing 68 (2016) 366–377.
[16] P. Pietrzak, M. Meller, M. Niedźwiecki, Dynamic mass measurement in checkweighers using a discrete time-variant low-pass filter, Mechanical Systems and Signal Processing 48 (1) (2014) 67 – 76.
[17] S. Almodarresi Yasin, N. White, Application of artificial neural networks to intelligent weighing systems, in: IEE Proceedings: Science, Measurement and Technology, Vol. 146, 1999, pp. 265–269.
[18] N. C. Singer, W. P. Seering, Preshaping command inputs to reduce system vibration, Journal of Dynamic Systems, Measurement and Control 112 (1) (1990) 76–82.
[19] D. Richiedei, A. Trevisani, Shaper-based filters for the compensation of the load cell response in dynamic mass measurement, Mechanical Systems and Signal Processing 98 (17) (2018) 281–291.
[20] J. S. Choi, Y. S. Baek, Magnetically-levitated steel-plate conveyance system using electromagnets and a linear induction motor, IEEE Transactions on Magnetics 44 (11) (2008) 4171–4174.
[21] L. Marko, M. Saxinger, A. Steinboeck, A. Kugi, Magnetic actuator design for strip stabilizers in hot dip galvanizing lines, in: Proceedings of the IEEE Industry Applications Society Annual Meeting, Portland, Oregon, USA, 2018, pp. 1–9.
[22] M. Saxinger, L. Marko, A. Steinboeck, A. Kugi, Active rejection control for unknown harmonic disturbances of the transverse deflection of steel strips with control input, system output, sensor output, and disturbance input at different positions, Mechatronics 56 (2018) 73 – 86.
[23] H. Bleuler, M. Cole, P. Keogh, R. Larsonneur, E. Maslen, R. Nordmann, Y. Okada, G. Schweitzer, A. Traxler, Magnetic Bearings, Springer, Dortrecht Heidelberg London New York, 2009.
[24] D. M. Stefanescu, Handbook of Force Transducers: Principles and Components, Springer, Berlin Heidelberg, 2011.
[25] G. Gautschi, Piezoelectric Sensorics: Force Strain Pressure Acceleration and Acoustic Emission Sensors Materials and Amplifiers, Springer, Berlin Heidelberg, 2002.
[26] J.-J. E. Slotine, W. Li, Applied nonlinear control, Prentice Hall, Englewood Cliffs, New Jersey, 1991.
[27] G. F. Franklin, J. D. Powell, A. Emami-Naeini, Feedback Control of Dynamic Systems, 6th Edition, Pearson Higher Education, Upper Saddle River, New Jersey, 2009.
[28] B. Friedland, Limiting forms of optimum stochastic linear regulators, Journal of Dynamic Systems, Measurement, and Control 93 (3) (1971) 134–141.
[29] R. Feynman, R. Leighton, M. Sands, The Feynman Lectures on Physics, Vol. II: The New Millennium Edition: Mainly Electromagnetism and Matter, Basic Books, New York, 2011.

Post-print version of the article: U. Knechtelsdorfer, M. Saxinger, M. Schwegel, A. Steinboeck, and A. Kugi, "A two-stage observer for the compensation of actuator-induced disturbances in tool-force sensors", *Mechanical Systems and Signal Processing*, vol. 146, pp. 106989-1–106989-12, 2021, ISSN: 0888-3270. DOI: 10.1016/j.ymssp.2020.106989